Inorg. Chem. **2002**, *41*, 3410–3422

Construction of Hydrogen-Bonded and Coordination-Bonded Networks of Cobalt(II) with Pyromellitate: Synthesis, Structures, and Magnetic Properties

Hitoshi Kumagai,[†,‡] Cameron J. Kepert,[§] and Mohamedally Kurmoo*[,†]

Institut de Physique et Chimie des Matériaux de Strasbourg, 23 rue du Loess, 67037 Strasbourg Cedex, France, Applied Molecular Science, Institute for Molecular Science (IMS), Nishigounaka 38, Myoudaiji, Okazaki 444-8585, Japan, and Centre for Heavy Metals Research, School of Chemistry, University of Sydney, New South Wales 2006, Australia

Received January 23, 2002

Synthesis (hydrothermal and metathesis), characterization (UV–vis, IR, TG/DTA), single-crystal X-ray structures, and magnetic properties of three cobalt(II)–pyromellitate complexes, purple $[Co_2(pm)]_n$ (**1**), red $[Co_2(pm)(H_2O)_4]_n \cdot 2nH_2O$ (**2**), and pink $[Co(H_2O)_6](H_2pm)$ (**3**) (H_4pm = pyromellitic acid (1,2,4,5-benzenetetracarboxylic acid)), are described. **1** consists of one-dimensional chains of edge-sharing CoO_6 octahedra that are connected into layers via O–C–O bridges. The layers are held together by the pyromellitate (pm^{4-}) backbone to give a three-dimensional structure, each ligand participating in an unprecedented 12 coordination bonds (Co–O) to 10 cobalt atoms. **2** consists of a three-dimensional coordination network possessing cavities in which unbound water molecules reside. This highly symmetric network comprises eight coordinate bonds (Co–O) between oxygen atoms of pm^{4-} to six *trans*-$Co(H_2O)_2$. **3** possesses a hydrogen-bonded sandwich structure associating layers of $[Co(H_2O)_6]^{2+}$ and planar H_2pm^{2-}. The IR spectra, reflecting the different coordination modes and charges of the pyromellitate, are presented and discussed. The magnetic properties of **1** indicate complex behavior with three ground states (collinear and canted antiferromagnetism and field-induced ferromagnetism). Above the Néel temperature (T_N) of 16 K it displays paramagnetism with short-range ferromagnetic interactions (Θ = +16.4 K, μ_{eff} = 4.90 μ_B per Co). Below T_N a weak spontaneous magnetization is observed at 12.8 K in low applied fields (H < 100 Oe). At higher fields (H > 1000 Oe) metamagnetic behavior is observed. Two types of hysteresis loops are observed; one centered about zero field and the second about the metamagnetic critical field. The critical field and the hysteresis width increase as the temperature is lowered. The heat capacity data suggest that **1** has a 2D or 3D magnetic lattice, and the derived magnetic entropy data confirm an anisotropic $s_{eff} = {}^1/_2$ for the cobalt(II) ion. Magnetic susceptibility data indicate that **2** and **3** are paramagnets.

Introduction

The synthesis of metal−organic hybrid compounds by metal ion directed assembly of organic molecular building blocks (i.e. tectons) using the concept of supramolecular engineering represents one of the most active research areas in chemistry and materials science.[1] The wide interest in these materials is driven by their collective properties, such as magnetism and electrical conduction, and their potential technological applications.[2] The metal−organic hybrids present the unique possibility of combining the properties associated with these individual components in one hybrid compound.[3,4] The rare existence of superconductivity in the presence of very dense inorganic paramagnetic layers in the hybrid compound $(BEDT\text{-}TTF)_4((H_3O)Fe(C_2O_4)_3).C_6H_5CN$ (where BEDT-TTF is bis(ethylenedithio)tetrathiafulvalene) has been demonstrated.[4] The combination of nonlinear optical activity and magnetism is also under investigation.[5] Furthermore, due to the porous and/or layered nature in some cases, there is increasing interest in selective sorption, host−guest chemistry, and catalysis.[6,7] However, the combination of structural properties such as porosity with any of these

* To whom correspondence should be addressed. E-mail: kurmoo@ipcms.u-strasbg.fr.
[†] Institut de Physique et Chimie des Matériaux de Strasbourg.
[‡] Institute for Molecular Science.
[§] University of Sydney.

10.1021/ic020065y CCC: $22.00
Published on Web 05/30/2002

physical properties is rare.[8] It is generally believed that there should be some orbital overlap between the nearest neighboring centers, whether organic radicals or metal ions, to generate conduction bands for electrical conductivity or long-range magnetic orderings.[9,10] This requirement and the presence of pores are therefore difficult to achieve spatially in one material. Given the long list of applications of porous materials, such as gas sorption, catalysis, drug delivery, separations, etc., they would be even more powerful agents if, in addition to their pores, they possessed another property such as magnetism.

In line with our recent study of long-range magnetic ordering in low-dimensional metal complexes, we have been trying to develop metal−carboxylate hybrid materials and have found a number of low-dimensional magnets.[11,12] These compounds can be divided into three groups; the first group is layered and behaves as a ferrimagnet with a Curie temperature reaching 60 K and coercive fields approaching 20 kOe,[11] and the second group is also layered and behaves as metamagnets with very strong anisotropy that results in a coercive field in excess of 50 kOe at 2 K.[12] The third group has one-dimensional chains and exhibits unusual magnetic behaviors.[13]

Tri- and tetracarboxylates as multiconnecting ligands are also excellent candidates for the synthesis of hybrid materials.[14] We reported two types of cobaltous tricarboxylate compounds: one is a series of molecular cavities constructed from aromatic BTC (BTC = 1,3,5-benzenetricarboxylate), and the other is a coordination polymer of nonaromatic CTC (CTC = 1,3,5-cyclohexanetricarboxylate).[7,15] For BTC, none of the networks to have been characterized structurally have been shown to display long-range magnetic ordering. There is only one example that exhibits long-range ordering, but its structure is not reported.[16] On the other hand, CTC

(1) (a) Day, P., Gillespie, R. *Philos. Trans. R. Soc. London, Ser. A* **1985**, *A314*. (b) Cotton, F. A.; Lin, C.; Murillo, C. A. *Acc. Chem. Res.* **2001**, *34*, 759. (c) Day, P. *J. Chem. Soc., Dalton Trans.* **2000**, 3483. (d) Fujita, M., Ed. Molecular Self-Assembly, Organic versus Inorganic Approaches. *Struct. Bonding* **2000**, *96*. (e) Lehn, J.-M. *Supramolecular Chemistry, Concepts and Perspectives*; VCH: Weinheim, Germany, 1995. (f) Hosseini, M. W. *New J. Chem*. **1998**, *22*, 87 (special issue on molecular networks). (g) Sauvage, J.-P., Dietrich-Buchecker, C., Eds. *Molecular Catenanes, Rotaxanes and Knots: A Journey Through the World of Molecular Topology*; Wiley-VCH: Weinheim, Germany, 1999. (h) Leininger, S.; Olenyuk, B.; Stang, P. J. *Chem. Rev*. **2000**, *100*, 853. (i) Beer, P. D., Ed. *Transition Metals in Supramlecular Chemistry*; Kluwer: Dordrecht, The Netherlands, 1994. (j) Robson, R.; Batten, S. R. *Angew. Chem., Int. Ed*. **1998**, *37*, 1460. (k) O'Hare, D., Bruce, D. W. Eds. *Inorganic Materials*; Wiley: Chichester, U.K., 1992.

(2) (a) Day, P., Underhill, A. E., Eds. Metal-Organic and Organic Molecular Magnets. *Philos. Trans. R. Soc. London* **1999**, *357*. (b) Kahn, O., Ed. *Magnetism: A Supramolecular Function*; Kluwer Academic: Dordrecht, The Netherlands, 1996. (c) Kahn, O. *Acc. Chem. Res.* **2000**, *33*, 647. (d) Veciana, J., Rovira, C., Amabilino, D. B., Eds. *Supramolecular Engineering of Synthetic Metallic Materials, Conductors and Magnets*; NATO ASI Series C518; Kluwer Academic: Dordrecht, The Netherlands, 1998. (e) Itoh, K., Kinoshita, M., Eds. *Molecular Magnetism, New Magnetic Materials*; Gordon and Breach-Kodansha: Tokyo, 2000.

(3) (a) Day, P.; Kurmoo, M.; Mallah, T.; Marsden, I. R.; Friend, R. H.; Pratt, F. L.; Hayes, W.; Chasseau, D.; Gaultier, J.; Bravic, G.; Ducasse, L. *J. Am. Chem. Soc.* **1992**, *114*, 10722. (b) Kobayashi, H.; Sato, A.; Arai, E.; Akutsu, H.; Kobayashi, A.; Cassoux, P. *J. Am. Chem. Soc.* **1997**, *119*, 12392. (c) Kobayashi, H.; Tomita, H.; Naito, T.; Kobayashi, A.; Sakai, F.; Watanabe, T.; Cassoux, P. *J. Am. Chem. Soc*. **1996**, *118*, 368. (d) Marsden, I. R.; Allan, M. L.; Friend, R. H.; Kurmoo, M.; Kanazawa, D.; Day, P.; Chasseau, D.; Bravic, G.; Ducasse, L. *Phys. Rev.* **1994**, *B50*, 2118. (e) Day, P.; Kurmoo, M.; *J. Mater. Chem.* **1997**, *7*, 1291−1295. (f) Coronado, E.; Galan-Mascaros, J. R.; Laukhin, V. *Nature* **2000**, *408*, 447. (g) Coronado, T.; Gomez-Gracia, C. J. *Chem. Rev.* **1998**, *98*, 273.

(4) Kurmoo, M.; Graham, A. W.; Day, P.; Coles, S. J.; Hursthouse, M. B.; Caulfield, J. L.; Singleton, J.; Francis, J. P.; Hayes, W.; Ducasse, L.; Guionneau, P. *J. Am. Chem. Soc*. **1995**, *117*, 12209.

(5) (a) Sugano, S., Kojima, N., Eds. *Magnetooptics*; Springer-Verlag: Berlin, 2000. (b) Benard, S.; Yu, P.; Audiere, J. P.; Riviere, E.; Clement, R.; Guilhem, J.; Tchertanov, L.; Nakatani, K. *J. Am. Chem. Soc.* **2000**, *122*, 9444. (c) Lacroix, P. G. *Eur. J. Inorg. Chem.* **2001**, 339. (d) Lacroix, P. G.; Clement, R.; Nakatani, K.; Zyss, J.; Ledoux, I. *Science* **1994**, *263*, 658. (e) Sato, O.; Iyoda, T.; Fujishima, A.; Hashimoto, K. *Science* **1996**, *271*, 49.

(6) (a) Lagaly, G. *Appl. Clay Sci.* **1999**, *15*, 1. (b) Barton, T. J.; Bull, L. M.; Klemperer, W. G.; Loy, D. A.; McEnaney, B.; Misono, M.; Monson, P. A.; Pez, G.; Scherer, G. W.; Vartuli, J. C.; Yaghi, O. M. *Chem. Mater*. **1999**, *2633*, 3. (c) O'Keeffe, M.; Eddaoudi, M.; Li, H.; Reineke, T.; Yaghi, O. M. *J. Solid State Chem.* **2000**, *152*, 3. (d) Yaghi, O. M.; Li, H.; Davis, C.; Richardson, D.; Groy, T. L. *Acc. Chem. Res.* **1998**, *31*, 474. (e) Kitagawa, S.; Kondo, M. *Bull. Chem. Soc. Jpn*. **1998**, *71*, 1739. (f) Kawata, S.; Kitagawa, S.; Kumagai, H.; Kudo, C.; Kamesaki, H.; Ishiyama, T.; Kondo, M.; Katada, M. *Inorg. Chem.* **1996**, *35*, 4449. (g) Kawata, S.; Kitagawa, S.; Kumagai, H.; Ishiyama, T.; Honda, K.; Tobita, H.; Adachi, K.; Katada, M. *Chem. Mater*. **1998**, *10*, 3902.

(7) (a) Kepert, C. J.; Prior, T. J.; Rosseinsky, M. J. *J. Am. Chem. Soc*. **2000**, *122*, 5158. (b) Kepert, C. J.; Prior, T. J.; Rosseinsky, M. J. *J. Solid State Chem.* **2000**, *152*, 261. (c) Kepert, C. J.; Rosseinsky, M. J. *Chem. Commun.* **1998**, 31. (d) Kepert, C. J.; Hesek, D.; Beer, P. D.; Rosseinsky, M. J. *Angew. Chem., Int. Ed*. **1998**, *37*, 3158.

(8) (a) Rujiwatra, A.; Kepert, C. J.; Rosseinsky, M. J. *Chem. Commun*. **1999**, 2307. (b) Rujiwatra, A.; Kepert, C. J.; Claridge, J. B.; Rosseinsky, M. J.; Kumagai, H.; Kurmoo, M. *J. Am. Chem. Soc.* **2001**, *123*, 10584.

(9) Ishiguro, T.; Yamaji, K.; Saito, G. *Organic Superconductors*, 2nd ed.; Springer-Verlag: Berlin, 1998.

(10) Aharony, A. *Introduction to the Theory of Ferromagnetism*; Oxford Science Publications, Clarendon Press: Oxford, U.K., 1996.

(11) (a) Kurmoo, M. *Chem. Mater*. **1999**, *11*, 3370. (b) Kurmoo, M.; Day, P.; Derory, A.; Estournes, C.; Poinsot, R.; Stead, M. J.; Kepert, C. J. *J. Solid State Chem.* **1999**, *145*, 452. (c) Kurmoo, M. *J. Mater. Chem.* **1999**, *9*, 2595. (d) Kurmoo, M. *Mol. Cryst. Liq. Cryst.* **2000**, *342*, 167. (e) Kurmoo, M. *Mol. Cryst. Liq. Cryst.* **2000**, *341*, 395.

(12) (a) Kurmoo, M. *Philos. Trans. R. Soc. London, Ser. A* **1999**, *357*, 3041. (b) Kurmoo, M.; Kumagai, H.; Green, M. A.; Lovett, B. W.; Blundell, S. J.; Ardavan, A.; Singleton, J. *J. Solid State Chem.* **2001**, *159*, 343. (c) Kurmoo, M.; Kumagai, H. *Mol. Cryst. Liq. Cryst*. **2002**, *376*, 555.

(13) Kurmoo, M.; Kumagai, H. Unpublished results.

(14) (a) Chu, D.-Q.; Xu, J.-Q.; Duan, L.-M.; Wang, T.-G.; Tang, A.-Q.; Ye, L. *Eur. J. Inorg. Chem.* **2001**, 1135. (b) Yaghi, O. M.; Jernigan, R.; Li, H.; Davis, C. E.; Groy, T. L. *J. Chem. Soc., Dalton Trans.* **1997**, 2383. (c) Gutschke, G. O. H.; Molinier, M.; Powell, A. K.; Winpenny, R. E. P.; Wood, P. T. *Chem. Commun.* **1996**, 823. (d) Guillou, N.; Livage, C.; Marrot, J.; Ferey, G. *Acta Crystallogr*. **2000**, *C56*, 1427. (e) Livage, C.; Guillou, N.; Marrot, J.; Ferey, G. *Chem. Mater*. **2001**, *13*, 4387. (f) Foreman, M. R. S. J.; Gelbrich, T.; Hursthouse, M. B.; Platter, M. J. *Inorg. Chem. Commun.* **2000**, *3*, 234. (g) Chui, S. S.-Y.; Lo, S. M.-F.; Charmant, J. P. H.; Orpen, A. G.; Williams, I. D. *Science* **1999**, *283*, 1148. (h) Platter, M. J.; Howie, R. A.; Roberts, A. J. *Chem. Commun.* **1997**, 893. (i) Platter, M. J.; Roberts, A. J.; Marr, J.; Lachowski, E. E.; Howie, R. A. *J. Chem. Soc., Dalton Trans.* **1998**, 797. (j) Platter, M. J.; Foreman, M. R. S. J.; Coronado, E.; Gomez-Garcia, C. J.; Slawin, A. M. Z. *J. Chem. Soc., Dalton Trans* **1999**, 4209. (k) Yaghi, O. M.; Li, H.; Groy, T. L. *J. Am. Chem. Soc.* **1996**, *118*, 9096. (l) Yaghi, O. M.; Davis, C. E.; Li, G.; Li, H. *J. Am. Chem. Soc.* **1997**, *119*, 2861. (m) Michaelides, A.; Skoulika, S.; Kirtsis, V.; Raotopoulou, C.; Terzis, A. *J. Chem. Res.* **1997**, 204.

(15) Kumagai, H.; Akita-Tanaka, M.; Inoue, K.; Kurmoo, M. *J. Mater. Chem*. **2001**, *11*, 2146.

(16) (a) Wynn, C. W.; Albrecht, A. S.; Landee, C. P.; Turnbull, M. M.; Dodrill, B. *J. Solid State Chem.* **2001**, *159*, 379. (b) Landee, C. P.; Wynn, C. M.; Albrecht, A. S.; Zhang, W.; Vunni, C. B.; Parent, J. L.; Navas, C.; Turnbull, M. M. *J. Appl. Phys*. **1994**, *75*, 5535. (c) Wynn, C. M.; Albrecht, A. S.; Landee, C. P.; Zhang, W.; Navas, C.; Turnbull, M. M. *Mol. Cryst. Liq. Cryst.* **1995**, *274*, 1.

Table 1. Summary of Known Metal−Pyromellitate Complexes and Their Multitopicities

compd	charge of pm	geometry of pm	no. of bonds	no. of connecting metals	ref
$[Co(H_2O)_6](H_2pm)$	2−	planar	0	0	25, 26, this work
$[Ni(H_2O)_6](H_2pm)$	2−	planar	0	0	21, 25
$[Mn(H_2O)_6](H_2pm)$	2−	planar	0	0	25
$Na_2Co(H_2O)_6(H_2pm)\cdot 4H_2O$	2−	planar	0	0	27
$\{Ni(en)(H_2O)_3\}_2(pm)\cdot 4H_2O$[a]	4−	nonplanar	2	2	28
$\{Ni(H_2O)_5\}_2(pm)\cdot 6H_2O$[a]	4−	nonplanar	2	2	25
$\{Mn(H_2O)_5\}_2(pm)\cdot H_2O$[a]	4−	nonplanar	2	2	29
$Co_2(pm)L_4$	4−	nonplanar	2	2	30
$\{Cu(dipn)(H_2O)\}_2(pm)\cdot 8H_2O$[a]	4−	nonplanar	2	2	31
$\{CuL(H_2O)\}_2(H_2pm)(ClO_4)_2$	2−	planar	4	2	32
$[Co(H_2O)_6][Co(H_2O)_4(pm)]\cdot nH_2O$[b]	4−	nonplanar	2	2	33
$Ca_2(pm)\cdot 6H_2O$[c]	4−	nonplanar	10	6	34
$Fe_2(phen)_2(pm)$[c]	4−	nonplanar	6	6	35
$[Cu_2(H_2O)_6(pm)]\cdot nH_2O$[c]	4−	nonplanar	4	4	36
[Cu(dien)Cu(dien)(H_2O)(pm)] $ClO_4\cdot H_2O$[c]	4−	nonplanar	6	6	31b
$Na_2Zn(pm)\cdot 9H_2O$[d]	4−	nonplanar	8	8	37
$Zn(H_2O)_5Zn(pm)\cdot 2H_2O$[d]	4−	nonplanar	6	5	38
$Ag_2(pm)$[d]	2−	nonplanar	10	10	23
$Co_5(OH)_2(pm)_2(H_2O)_4\cdot xH_2O$[e]	4−	nonplanar	10	10	39
$[Co_2(H_2O)_4(pm)]\cdot 2H_2O$[d]	4−	nonplanar	8	6	this work
$Co_2(pm)$[d]	4−	nonplanar	12	10	this work

[a] Dimer. [b] Chain. [c] Layer. [d] Three-dimensional. [e] Three-dimensional based on a bow-tie $Co_5(OH)_2$ pentamer.

generates open-framework structures with sizable channels and behaves as short-range coupled low-dimensional chains with a tendency for ferrimagnetic alignment.[15] Our present investigation focuses on the use of pyromellitic acid (1,2,4,5-benzenetetracarboxylic acid or H_4pm) as a structural building block in the synthesis of metal−organic hybrid materials. We have employed the technique of hydrothermal synthesis, which is well suited to the preparation of crystals of synthetic minerals, new inorganic materials, and metal−organic framework polymers.[17] Here we report the hydrothermal synthesis, single-crystal structures, and magnetic properties of three Co(II)−pyromellitate compounds.

Pyromellitic acid is an important raw material for the plastics industry. The purely organic plastic made from it is being increasingly used in aerospace technology due to its excellent thermal and mechanical properties.[18] It is also used for separating lanthanides from solutions containing Mg^{II}, Co^{II}, Mn^{II}, etc., due to its multidentate nature, and as an eluent for ion chromatography.[19]

Pyromellitic acid consists of a rigid planar C_{10} backbone due to the π-bonding of the benzene ring and four freely rotating and flexible carboxylate groups.[20] It can be deprotonated to give four available charges (1− to 4−), although the 2− and 4− anions are most commonly found and a rare case of a 1− anion is known in the tetrabutylammonium salt.[21] No example of a 3− anion is known to date. In the partially deprotonated forms it exhibits intramolecular hydrogen bonds between carboxylate and carboxylic acid.[21,22] Consequently, the hydrogen-bonded pair becomes coplanar with the C_{10} backbone. All known examples of 2− anions are planar, with the exception of the ammonium salt, due to the presence of intermolecular cation−anion hydrogen bonds, and the silver salt.[21,23] The acid is also nonplanar in its hydrated crystal form.[20] All known examples containing the 4− anion are nonplanar.

Pyromellitic acid has been used for the study of hydrogen bonding in supramolecular organic networks.[24] A wide range of coordination complexes is known with transition metals and some with lanthanides that were prepared by reaction in aqueous solutions. The known compounds (Table 1) have dimeric units bridged by either H_2pm^{2-} or $pm,^{4-}$ a one-dimensional chain structure with bridging pm^{4-}, a square grid of two-dimensional layers with bridging pm^{4-}, and three-dimensional architectures with bridging pm^{4-}.[25−39] In some cases of the latter the structures have cavities and channels

(17) (a) Lieth, R. M. A. *Preparation and Crystal Growth of Materials with Layered Structure*; Plenum: New York, 1997. (b) Price, D. J.; Powell, A. K.; Wood, P. T. *J. Chem. Soc., Dalton Trans.* **2000**, 3566. (c) Price, D. J.; Lionti, F.; Ballou, R.; Wood, P. T.; Powell, A. K. *Philos. Trans. R. Soc. London, Ser. A* **1999**, *357*, 3099. (d) Hagrman, P. J.; Hagrman, D.; Zubieta, J. *Angew. Chem., Int. Ed.* **1999**, *38*, 2638. (e) Maschmeyer, T.; Rey, F.; Sankar, G.; Thomas, J. M. *Nature* **1995**, *378*, 159. (f) Bu, X.; Feng, P.; Stucky, G. D. *J. Solid State Chem.* **1997**, *131*, 387. (g) Clearfield, A. In *Inorganic Ion Exchange Materials;* Clearfield, A., Ed.; CRC Press: Boca Raton, FL, 1991.

(18) Inoue, T.; Kumagai, Y.; Kakimoto, M.-A.; Imai, Y.; Watanabe, J. *Macromolecules* **1997**, *30*, 1921.

(19) Ohta, K.; Tanaka, K. *J. Chromatogr. A* **1998**, *804*, 87.

(20) Takusagawa, F.; Hirotsu, K.; Shimada, A. *Bull. Chem. Soc. Jpn.* **1971**, *44*, 1274.

(21) Jensen, S. M.; Küppers, H.; Luehrs, *Z. Naturforsch., B* **1992**, *47b*, 1141.

(22) Jessen, S. M.; Küppers, H. *Acta Crystallogr.* **1990**, *C46*, 2351.

(23) Jaber, F.; Charbonnier, F.; Faure, R. *J. Chem. Cryst.* **1997**, *27*, 397.

(24) (a) Felix, O.; Hosseini, M. W.; De Cian, A. *Solid State Sci.* **2001**, 3, 789. (b) Biranda, K.; Zaworotko, M. J. *Cryst. Eng.* **1998**, *1*, 67. (c) Mrvos-Sermek, D.; Popovic, Z.; Matkovic-Calogovic, D. *Acta Crystallogr.* **1996**, *C52*, 2538. (d) Desiraju, G. R. *Angew. Chem., Int. Ed. Engl.* **1995**, *34*, 2311. (e) Desiraju, G. R.; Steiner, T. *The Weak Hydrogen Bond in Structural Chemistry and Biology*; IUCr Monograph on Crystallography 9; Oxford University Press: Oxford, U.K., 1999. (f) Lough, A. J.; Wheatley, P. S.; Ferguson, G.; Glidewell, C. *Acta Crystallogr.* **2000**, *B56*, 261.

(25) Rochon, F. D.; Massarweh, G. *Inorg. Chim. Acta* **2000**, *304*, 190.

(26) Ward, D. L.; Luehrs, D. C. *Acta Crystallogr.* **1983**, *C39*, 1370.

(27) Karanovic, L.; Poleti, D.; Bogdanovic, G. A.; Spasojevic-de Bire, A. *Acta Crystallogr.* **1999**, *C55*, 911.

(28) Poleti, D.; Stojakovic, D. R.; Prelesnik, B. V.; Herak, R. M. *Acta Crystallogr.* **1988**, *C44*, 242.

(29) Cheng, D.; Zheng, Y.; Li, J.; Xu, D.; Xu, Y. *Acta Crystallogr.* **2000**, *C56*, 523.

Chart 1. Modes of Coordination of the Carboxylate Ion and the Coordination Modes Observed in **1** and **2**

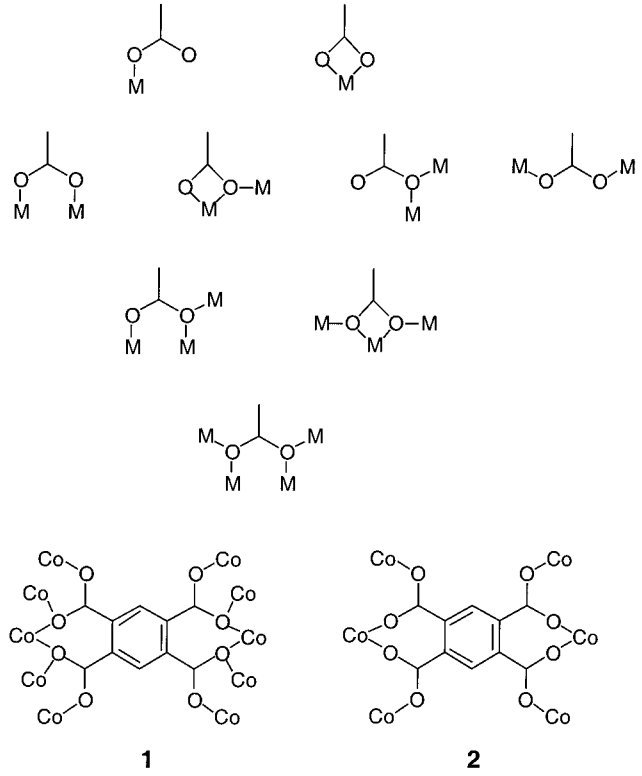

which are filled with water. Only one example of a hydrothermally prepared complex is known to date.[39]

As with most carboxylates, pyromellitate provides several possible coordination modes, viz. unidentate, bis-unidentate, bidentate, and tridentate, of the independent carboxylate groups (Chart 1). In addition, it can also chelate via one carboxylate group or via the oxygen atoms of neighboring carboxylate groups (for example, those in the 1- and 2-positions of the benzene ring). Its known multitopicity, that is, the number of coordinate bonds to the number of metals, can vary from 2 to 10 coordination bonds and it can coordinate to up to 10 metals, as in the case of Ca and Ag, or 6 in the Zn salt (Table 1). In the present study we found two examples that extend these limits; one compound coordinates through 8 bonds to 6 metals, and the other shows an unprecedented 12 bonds to 10 metals.

(30) (a) Li, Y.-T.; Yan, C.-W, *Synth. React. Inorg. Met.-Org. Chem.* **2000**, *30*(6), 1069. (b) Yan, C.-W.; Li, Y.-T.; Liao, D.-Z. *Chin. J. Chem.* **2000**, *18*(3), 351. (c) Li, Y.-T.; Yan, C.-W.; Kong, X.-H. *Pol. J. Chem.* **1999**, *73*(10), 1665.

(31) (a) Chen, W.; Tioh, N. H.; Zou, J.-Z.; Xu, Z.; You, X. Z. *Acta Crystallogr.* **1996**, *C52*, 43. (b) Zou, J.-Z.; Liu, Q.; Xu, Z.; You, X. Z.; Huang, X.-Y. *Polyhedron* **1998**, *17*, 1863.

(32) Chaudhuri, P.; Oder, K.; Weighardt, K.; Gehring, S.; Haase, W.; Nuber, B. *J. Am. Chem. Soc.* **1988**, *100*, 3657.

(33) (a) Robl, C.; Hentechel, S. *Mater. Res. Bull.* **1991**, *26*, 1355. (b) Poleti, D.; Karanovic, Lj. *Acta Crystallogr.* **1989**, *C45*, 1716.

(34) Robl, C. *Z. Naturforsch., B* **1988**, *B43*, 993.

(35) Chu, D.-Q.; Xu, J.-Q.; Duan, L.-M.; Wang, T.-G.; Tang, A.-Q.; Ye, L. *Eur. J. Inorg. Chem.* **2001**, 1135.

(36) Usubaliev, B. T.; Shnulin, A. N.; Mamadov, H. S. *Koord. Khim.* **1983**, *8*, 1532.

(37) Robl, C. *Mater. Res. Bull.* **1992**, *27*, 99.

(38) Robl, C. *Z. Anorg. Allg. Chem.* **1987**, *554*, 79.

(39) Gutschke, S. O. H.; Price, D. J.; Powell, A. K.; Wood, P. T. *Eur. J. Inorg. Chem.* **2001**, 2739.

Our choice of cobalt for this study is due to (a) its variable coordination numbers (4−6), (b) its flexibility in forming coordination bonds in a wide range of lengths (1.9−2.4 Å), (c) its stability in air, (d) its high spin state in the weak crystal field of carboxylates, (e) its large orbital moment through a sizable spin−orbit coupling, (f) its magneto-crystalline anisotropy, which gives rise to high coercivity, and (g) its different colors.

Experimental Section

Synthesis. All chemicals were obtained from Aldrich and Fluka and used without further purification.

Preparation of Co_2(pm) (1). $Co(OH)_2$ (0.12 g, 1.3 mmol) was suspended in distilled water (ca. 30 mL), and a solution of H_4pm (0.25 g, 1.3 mmol) in distilled water (ca. 30 mL) was added. The mixture was placed in the Teflon liner of an autoclave, which was sealed and heated to 170 °C for 6 days. The mixture was then quenched in a water bath and cooled to room temperature for 2−3 h. Only violet crystals of **1** were obtained, which were filtered off, washed with water and acetone, and dried in air. Yield: 60%. Anal. Calcd for $Co_2O_8C_{10}H_2$: C, 32.64; H, 0.55. Found: C, 32.04; H, 0.80. IR bands (cm^{-1}): 447 m, 470 m, 553 s, 620 s, 637 s, 772 s, 805 s, 842 m, 862 m, 940 m, 1136 w, 1163 w, 1272 sh, 1305 m, 1360 vs, 1402 ssh, 1487 s, 1572 sbr, 1880 w.

This compound was also obtained from $CoCl_2 \cdot 6H_2O$ and $Co(NO_3)_2 \cdot 6H_2O$ as starting materials.

Preparation of $[Co_2(pm)(H_2O)_4]_n \cdot 2nH_2O$ (2). $CoCl_2 \cdot 6H_2O$ (1.0 g, 4.2 mmol) was dissolved in distilled water (ca. 30 mL) and a solution of H_4pm (0.53 g, 2.8 mmol) and NaOH (0.27 g, 6.7 mmol) in distilled water (ca. 30 mL) was added. The mixture was placed in the Teflon liner of an autoclave, sealed, and heated to 110 °C for 3 days. It was quenched and cooled to room temperature in a water bath for 3 h. Only the red crystals of **2** were obtained, which were filtered off, washed with water and acetone, and dried in air. Yield: 75%. Anal. Calcd for $Co_2O_{14}C_{10}H_{14}$: C, 25.23; H, 2.96. Found: C, 24.91; H, 2.96. IR bands (cm^{-1}): 485 w, 540 w, 586 w, 669 w, 745 w, 809 w, 839 vw, 879 w, 924 w, 1099 w, 1143 m, 1156 sh, 1285 m, 1330 sh, 1356 sh, 1398 s, 1440 m, 1501 m, 1558, 1584, 1606 s, 1662 m, 3270 ssh, 3410 vs, 3480 ssh, 3640 w.

Preparation of $[Co(H_2O)_6](H_2$pm) (3). This compound was obtained by two methods.

Method A. $[Co(H_2O)_6](NO_3)_2$ (3.0 g, 10.3 mmol) was dissolved in distilled water (ca. 30 mL), and a solution of H_4pm (1.31 g, 7 mmol) in distilled water (ca. 30 mL) was added. The mixture was placed in the Teflon liner of an autoclave, which was sealed and heated to 220 °C for 24 h. The mixture was then quenched and cooled to room temperature in a water bath for approximately 3 h. The violet crystals of **1** and pink crystals of **3** were filtered off, washed with water and acetone, and dried in air. The crystals of **3** were separated manually under an optical microscope. Yield: 20%. Anal. Calcd for $CoO_{14}C_{10}H_{16}$: C, 28.66; H, 3.85. Found: C, 28.68; H, 3.96.

Method B. $[Co(H_2O)_6](NO_3)_2$ (0.6 g, 2.1 mmol) and H_4pm (0.25 g, 1.3 mmol) were dissolved in distilled water (ca. 20 mL) and refluxed for 20 min. The solution was cooled slowly to room temperature, and the pink crystals were harvested after 6 h. The crystals were dried in air. Yield: 80%. Anal. Calcd for $CoO_{14}C_{10}H_{16}$: C, 28.66; H, 3.85. Found: C, 28.78; H, 4.03. IR bands: 552 brm, 640 w, 708 m, 745 m, 796 w, 888 w, 948 w, 1040 w, 1100 m, 1155 s, 1284 m, 1330 sh, 1352 s, 1515 s, 1587 s, 1665 s, 3272 ssh, 3426 vs.

PXRD and infrared spectroscopy indicate that the crystals from the two preparations are isostructural.

General Characterization. X-ray powder diffraction data were recorded at room temperature on a Siemens D-500 diffractometer equipped with graphite-monochromated Co Kα_1 (λ = 1.789 Å) radiation using the Bragg−Brentano geometry. Infrared spectra were recorded on a Mattson FTIR instrument by transmission through fine particles, prepared by crushing selected crystals, deposited on a KBr plate. UV−vis spectra were obtained by transmission through the compound dispersed in oil on a Hitachi U-3000 spectrometer. Thermogravimetry and differential thermal analysis (TG-DTA) were performed at rate of 5 °C/min in the temperature range 20−900 °C in air on a SETARAM system. Data were corrected for the empty platinum crucible. BET sorption−desorption of nitrogen and argon were studied on a FISONS Instruments Sorptomatic 1990 instrument.

Magnetic Measurements. The magnetic measurements of the complexes were carried out by use of Quantum Design MPMS-XL SQUID magnetometers in the temperature range 2−300 K and fields up to 5 T. Samples were fixed in gelatin capsules and held in drinking straws. Several temperature and field protocols were employed and will be described in the appropriate result section. For isothermal magnetization measurements of **1**, crystals were suspended in a solution of poly(methyl methacrylate) (PMMA) in CH_2Cl_2 and the solvent was evaporated to dryness, thus leaving the crystals fixed in the solid polymer. This technique prevents any torque of the crystallites in a magnetic field.

The phase diagram was studied by measuring the virgin magnetization after zero-field cooling from 30 K to the desired temperatures by use of a Princeton Applied Research Vibrating Sample magnetometer, Model 155. Variable-temperature measurements were performed in a continuous-flow cryostat, and the temperature of the sample was controlled by an ITC4 instrument (Oxford Instruments). Samples were tightly fixed in Perspex containers to prevent motion of the powder on ramping up the field.

Heat capacity was measured on a pressed pellet of **1** (ca. 200 mg) wrapped in a piece of aluminum foil in the range 1.6−38 K. Data were taken by employing a pseudo-adiabatic technique and corrected for the sample holder.

X-ray Crystallography and Structure Solution. A crystal of **1** was mounted in a thin film of perfluoropolyether oil on mohair fiber, and data were collected at 150 K on a Bruker SMART 1000 CCD instrument at the University of Sydney. Single crystals of **2** and **3** were glued on the tips of glass fibers, and data were collected at 295 K on a Kappa CCD Nonius diffractometer at the Service de Cristallographie in Strasbourg. Both diffractometers employ graphite-monochromated Mo Kα (0.7107 Å) radiation. The data were corrected for Lorentz and polarization effects. The structures were solved by direct methods and expanded using Fourier techniques.[40] The non-hydrogen atoms were refined anisotropically. No extinction corrections have been applied. Full-matrix least-squares refinement on F_o^2 converged to $R = \sum||F_o| - |F_c||/\sum|F_o|$ and $R_w = [\sum w(|F_o| - |F_c|)^2/\sum w|F_o|^2]^{1/2}$, as given in Table 2.

The crystallographic data have been deposited at the Cambridge Crystallographic Data Centre and have been given the reference numbers 177567−177569.

(40) (a) Sheldrick, G. M. SHELXS-86 and SHELXL-93, Programs for the Solution and Refinement of Crystal Structures; University of Göttingen, Göttingen, Germany, 1986 and 1993. (b) Burla, M. C.; Camalli, M.; Cascarano, G.; Giacovazzo, C.; Polidori, G.; Spagna, R.; Viterbo, D. *J. Appl. Crystallogr*. **1989**, *22*, 389.

Table 2. Summary of the Crystallographic Data of the Complexes

	1	**2**	**3**
formula	CoC_5HO_4	$Co_2C_{10}H_{14}O_{14}$	$CoC_{10}H_{16}O_{14}$
mol wt	183.99	476.08	419.16
cryst syst	monoclinic	triclinic	monoclinic
space group	*C*2/*m*	$P\bar{1}$	*P*2/*n*
a (Å)	6.1269(12)	7.4383(4)	6.5384(4)
b (Å)	17.476(3)	8.8006(5)	9.9260(4)
c (Å)	4.5541(9)	12.4710(8)	11.7734(8)
α (deg)		100.605(5)	
β (deg)	115.531(3)	91.564(5)	94.722(5)
γ (deg)		92.844(5)	
V (Å^3)	440.01(15)	800.89(8)	761.5(1)
Z	4	2	2
D_c (g cm^{-3})	2.777	1.97	1.83
λ (Å)	0.7107	0.7107	0.7107
T/K	150	295	295
μ(Mo Kα) (cm^{-1})	3.816	2.147	1.206
no. of rflns	509 (463 > 2σ)	3640 (1563 > 3σ)	1852 (912 > 3σ)
goodness of fit	1.112	1.091	1.049
R (R_w)[a]	0.0292 (0.0714)	0.048 (0.069)	0.046 (0.063)
residual (e/Å^3)	+0.72/−0.474	+0.697/−0.918	+0.553/−0.616

[a] $R = \sum||F_o| - |F_c||/\sum|F_o|$; $R_w = [\sum w(|F_o| - |F_c|)^2/\sum w|F_o|^2]^{1/2}$.

Results and Discussion

Although the reaction of a divalent metal and a carboxylic acid appears simple, the range of compounds that can be obtained with pyromellitic acid, sometimes under the same experimental conditions, indicates this is not the case. The complexity can be seen in Table 1, where we have listed the known phases, the charge of the pyromellitate anion, and its modes of coordination, viz. the number of coordinate bonds to the number of metals. The range of phases is due to several factors: for example, (a) the different degrees of protonation of pyromellitate, (b) the planarity of the pyromellitate, (c) the different coordination modes of the carboxylate ion (Chart 1), (d) the intramolecular and intermolecular hydrogen bonding, and (e) the coordination numbers of the metal centers. The present observations together with previous ones indicate that there exist several phases of metal carboxylate which can be synthesized depending on the experimental conditions.

Structure and Spectroscopic Properties of $[Co_2(pm)]_n$ (1). The structure of **1** consists of only Co(II) and pyromellitate ligand, in contrast to the large water content of the other two structures of **2** and **3** (vide supra). An ORTEP drawing, the mode of coordination of the pm^{4-} anion, and selected bond distances and angles of **1** have been deposited as Supporting Information (Figure S1 and Table S1). The repeating structural motif is a dimer consisting of two edge-sharing symmetry-related Co(II) ions which are bridged by oxygen atoms of pyromellitate. The distance between the metal centers within the dimer is 3.36 Å. The structure (Figure 1) is formed of one-dimensional zigzag chains of these edge-sharing dimers of octahedral cobaltous ions, CoO_6, parallel to the *a* axis. The chains are connected to one another through O−C−O bridges to form layers parallel to the *ac* plane. The shortest interchain Co−O−C−O−Co distance is 4.47 Å. The benzene rings of the pyromellitate units connect the layers into a three-dimensional framework (Figure 1). The Co(II) ion sits on the crystallographic special

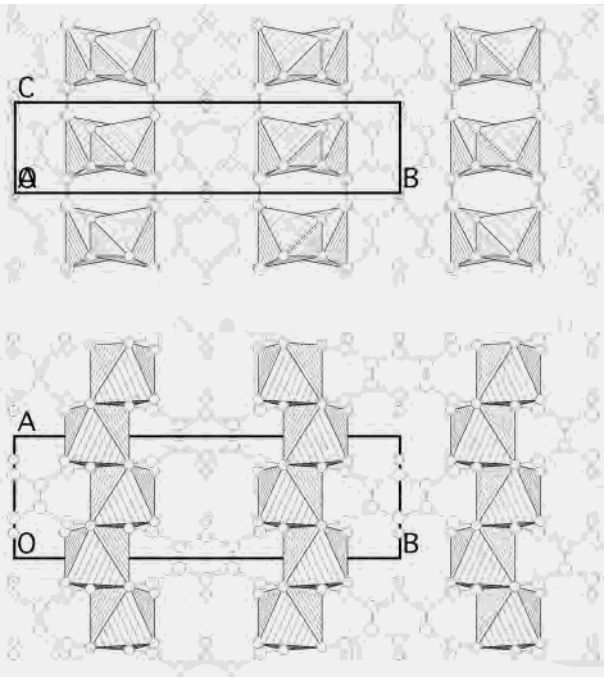

Figure 1. Projection of the structure of **1** along the (a, top) *a* axis and (b, bottom) *c* axis.

position and has three different bond lengths (2.029, 2.077, and 2.195 Å). The octahedra are not only distorted with regards to the distance of the oxygen atoms but also in bond angles. The distortions are characterized by bond angles of O(1)−Co(1)−O(2′), O(1′′)−Co(1)−O(2′′′) (159.0(1)°), and O(1′)−Co(1)−O(1′′) (170.6(1)°). The three-dimensional structure is reinforced by the presence of the strong Co−O coordination bonds with the pyromellitate units. The strong connections within a chain and between chains result in the striking thermal stability of this compound up to 320 °C. Despite their synthesis from aqueous solutions, the crystals of **1** show no evidence of water incorporation. The absence of trapped molecules was further confirmed by the result of the thermal analysis; the sample exhibited no weight loss up to 320 °C in air (Supporting Information, Figure S2) and decomposed at higher temperature, which is in good agreement with the elemental analysis, infrared spectrum, and X-ray crystallographic study. Furthermore, BET measurements on **1** gave a maximum absorption of either nitrogen or argon of 3 cm^2/g, suggesting no inclusion is possible, which was confirmed by calculating the void space using PLATON.[41] The stability for this metal carboxylate is comparable to those of MOF-5[42] and nickel succinate.[43]

1 exhibits a pseudo-triangular topology of the magnetic ions within the layer. The nearest distances between Co atoms are 3.368 Å between those in a chain and those connected via an oxygen atom and 4.475 and 4.554 Å for those between chains and those connected via O−C−O bridges. The distance between the layers is 8.788 Å, and the connection is via the pyromellitic backbone.

As already known from the chemistry of polycarboxylates such as BDC, CTC, and BTC (BDC = 1,4-benzenedicarboxylate, CTC = *cis,cis*-1,3,5-cyclohexanetricarboxylate, BTC = 1,3,5-benzenetricarboxylate), there is the possibility of having different coordination modes (Chart 1) of the carboxylate groups.[12,15] In compound **1**, we observe a coordination mode of the carboxylate moiety different from those found in **2** (Chart 1). Each carboxylate group coordinates to three cobalt atoms, as found in $Co_2(OH)_2$(terephthalate) and $[M_3(CTC)_2(\mu\text{-}H_2O)_2(H_2O)_2]\cdot 6H_2O$ (M = Ni, Co).[12,15] Three coordination bonds per carboxylate group of the pyromellitate ion satisfy the required coordination number of 6 for cobalt in Co_2pm. Consequently, there is no need for another coordinating ligand. This coordination mode therefore results in a multitopicity of 12 coordinate bonds to 10 metal atoms for the pyromellitate (Supporting Information, Figure S3). The number of coordination sites of the pyromellitate in compound **1** is, to our knowledge, the highest known (see Table 1).

It is interesting to consider the UV−vis spectrum of **1** because of its characteristic distorted coordination geometry (see Supporting Information, Figure S4). It is common for a Co(II) ion in octahedral coordination of weak ligands to have a red to pale pink coloration as in **2** and **3**, respectively, and to exhibit weak d−d absorption bands. Compound **1**, in contrast, has an intense violet color and displays dichroism under a polarizing microscope. Thin crystals have square platelike geometry and transmit dark blue in one polarization and light red in the other. The absorption spectrum exhibits three strong absorption bands in the visible region at 485, 508, and 580 nm. The last band also appears to be an overlap of two bands. The large splitting bands in the visible region and their enhanced intensities are in accordance with the large distortion from octahedral geometry of the metal center. The energies of the bands lie between those of Co(II) in an octahedral geometry (CoO_6) and a tetrahedral geometry (CoO_4).[44]

Crystal Structure of $[Co_2(pm)(H_2O)_4]_n\cdot 2nH_2O$ (2). The structure of **2** is shown in Figure 2. An ORTEP drawing of the structure around the cobalt ions with the atom-numbering scheme, a figure of the coordination mode of the pyromellitate, and selected bond distances and angles of **2** have been deposited as Supporting Information (Figure S5 and Table S2). The structure of **2** consists of three crystallographically independent Co(II) ions, two halves of the pyromellitate ligand, four coordinated water molecules, and two free water molecules. Co(2) and Co(3) ions are located on crystallographic special positions, and Co(1) lies on a general position. The crystal contains two crystallographically different pyromellitate ligands. Each cobalt atom adopts a distorted-octahedral geometry with water molecules in trans positions and four monodentate carboxylate groups in the basal plane. While Co(2) and Co(3) are symmetric due to

(41) Spek, A. L. *Acta Crystallogr*. **1990**, *A46*, C34.
(42) Li, H.; Eddouadi, M.; O'Keeffe, M.; Yaghi, O. M. *Nature* **1999**, *402*, 276.
(43) (a) Forster, P. M.; Cheetham, A. K. 13th International Zeolite Conference, Montpellier, France, July 8−13, 2001. (b) Forster, P. M.; Cheetham, A. K. *Angew. Chem., Int. Ed.* **2002**, *41*, 457.
(44) Lever, A. P. B. *Inorganic Electronic Spectroscopy*; Elsevier: Amsterdam, 1984.

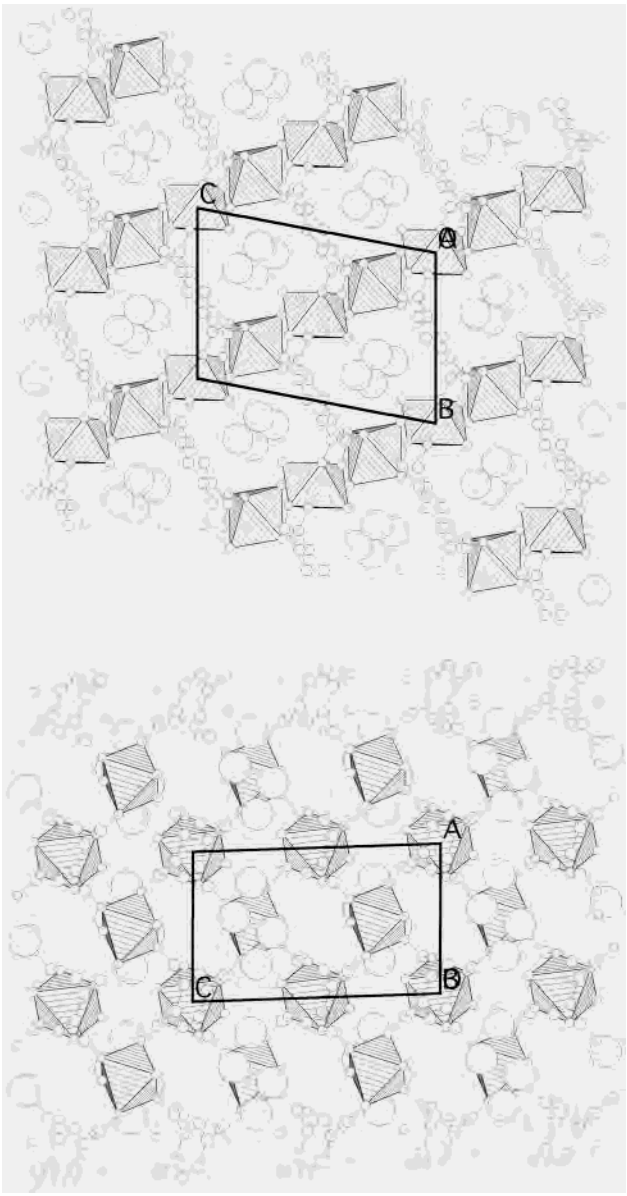

Figure 2. Projection of the structure of **2** along the (a, top) *a* axis and (b, bottom) *b* axis, showing the noncoordinated water molecules in the cavities. The hatched octahedra represent CoO_6 units, and the large circles represent the disordered water molecules.

their special positions, Co(1) is highly distorted. The first two exhibit an elongation of the Co−H_2O bonds (2.155 Å for Co(2) and 2.168 Å for Co(3)) compared to Co−O(carboxylate) (ranging between 2.033 and 2.059 Å). In contrast, for Co(1) the Co−OH_2 bond distances (2.108 Å) are shorter while the Co−O(carboxylate) bond distances are longer (ranging from 2.077 to 2.104 Å). The two independent pyromellitate units adopt a similar geometry with an almost planar C_{10} backbone, and the carboxylate oxygen atoms lie above and below it. The dihedral angles between benzene rings and the two different carboxylate moieties are 36 and 68°. This is in contrast with the planar pyromellitate dianion found in **3** (see below).

The overall structure is formed by octahedral cobaltous ions, CoO_6, which are connected to one another by O−C−O bridges[12,15] of the pyromellitate units to form a three-dimensional framework having sizable cavities (Figure 2). Alternatively, one can describe the structure as consisting of parallel zigzag chains of *trans*-Co(H_2O)$_2$ chelated by pyromellitate. The chains alternate, with one containing Co(2) and the other Co(3). These chains are then connected via the terminal carboxyl groups to Co(1) in a monodentate fashion to give the three-dimensional architecture.

The pyromellitate acts not only as a bidentate ligand to chelate Co(2) and Co(3) but also as a bridging ligand to connect Co(1) to Co(2) and Co(1) to Co(3) to give the polymeric structure (Chart 1 and the Supporting Information). The bite distance of the coordination oxygen atoms of neighboring carboxylates is 2.902 Å, longer than the hydrogen-bonded pair found in **3**. The chelating moiety forms a ring of seven atoms with the metal on coordination. The multitopicity of the pyromellitate is characterized by its eight coordinate bonds with six cobalt atoms (Supporting Information, Figure S6). This may be compared to the known examples listed in Table 1 and to the 1,3,5-cyclohexanetricarboxylate that forms six bonds to six metal atoms[15] and the terephthalate that forms six bonds with six metal atoms.[12] The size and shape of the pyromellitate ligand prevent any possible interpenetration of the lattice. The result is the high stability of a compound with cavities. These cavities are filled with water molecules (two per formula unit); their elevated temperature factors of the oxygen atoms and the lack of observation of their associated hydrogen atoms suggest that these molecules are fluctuating within the cavities and their mobility is limited by weak hydrogen bonds with the framework.

The metal atom layer has a pseudo-triangular topology with short Co−Co distances of 4.943 and 4.941 Å for Co(1)−Co(2) and Co(1)−Co(3), respectively, and 5.223 Å for those connected by O−C−O bridges and long distances of 6.932−7.432 Å for those which are not bridged.

It is worth commenting on the difference between the structures of **1** and **2**. Both compounds have the common unit of Co_2pm, with compound **2** having in addition six molecules of water per formula unit. Accordingly, there is a large difference between the calculated densities, of 2.78 g cm^{-3} for nonporous **1** and 1.97g cm^{-3} for porous **2**. The coordination linkages between metal sites also vary considerably, due to the presence of bound water. It is therefore not surprising that the structure of **1** is so stable up to 320 °C, due to the compactness and the large number of coordination bonds between anions and cations.

Crystal Structure of [Co(H_2O)$_6$](H_2pm) (3). The crystal belongs to the monoclinic system *P*2/*n*, with $a = 6.5384(4)$ Å, $b = 9.9260(4)$ Å, $c = 11.7734(8)$ Å, $\beta = 94.722(5)°$, $Z = 2$, and $V = 761.5(1)$ Å^3. Two other polymorphs have been reported and their lattice parameters are as follows: *P*2/*m*, $a = 6.530$ Å, $b = 9.930$ Å, $c = 6.508$ Å, $\beta = 115.48°$, $Z = 1$, $V = 381$ Å^3; *C*2/*c*, $a = 21.939$ Å, $b = 9.777$ Å, $c = 7.276$ Å, $\beta = 105.36°$, $Z = 4$, $V = 1505.0$ Å^3 (Table 1).[21,25,26] The asymmetric unit consists of one cobalt, half of a pyromellitate dianion (H_2pm^{2-}), and three water molecules which coordinate to the Co(II) ion. The adopted atom-numbering scheme, showing the geometry of the pyromellitate anion, and selected bond distances and angles of **3** have

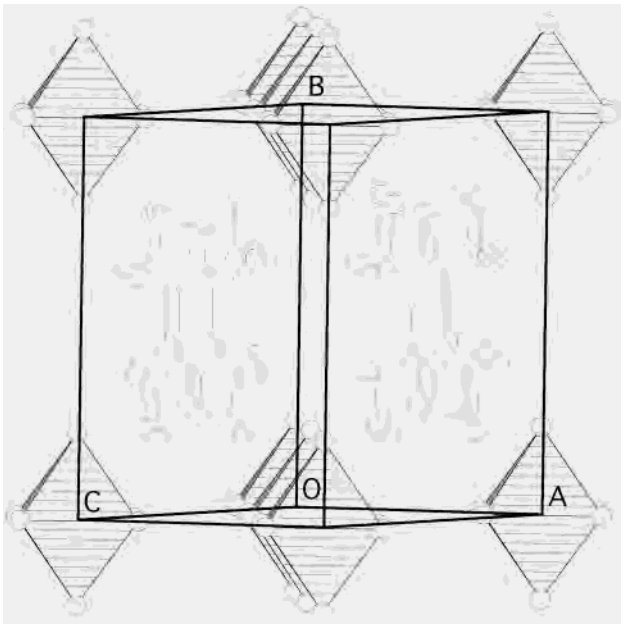

Figure 3. Structure of **3** showing layers of $Co(H_2O)_6^{2+}$ with planar H_2pm^{2-} in the gallery.

been deposited as Supporting Information (Figure S7 and Table S3). The structure consists of $[Co(H_2O)_6]^{2+}$ and pyromellitate dianion (Figure 3). The cobalt ion sits on a crystallographic special position and has octahedral coordination geometry, with the three Co−O bond lengths of 2.171, 2.073, and 2.047 Å. Magnetic susceptibility measurements (vide supra) confirm the oxidation state of the cobalt ion to be 2+. Pyromellitic acid (H_4pm) has four protons of carboxylate groups, which can give rise to four possible deprotonation steps. In the present case we found a dianion to balance the charge of the cation. The intermolecular hydrogen bonds between the protonated and deprotonated carboxylate groups force the pyromellitate dianion to be essentially planar.[21,22,24] The O−H···O distances between neighboring carboxylate groups is 2.383 Å. This is within the range of distances for those found in other pyromellitate and phthalate salts.[45] The torsional angles between the benzene ring (C(1)C(2)C(3)) and carboxylate groups (O(4)C(4)O(5) and O(6)C(5)O(7)) are 1.4(1)°. The angles of the benzene ring, 123.8, 118.8, and 117.3°, suggest a distorted geometry, although the ring remains planar. As the hydrogen atoms were not located in this structure, we noted that the distances between the coordinated water molecules and oxygen atoms of pyromellitate indicate the presence of hydrogen-bonding interactions to give the three-dimensional structure. The key structural motif of this compound is the layered structure of isolated $[Co(H_2O)_6]^{2+}$ in the *ac* plane separated by $(H_2pm)^{2-}$ along the *b* axis (Figure 3). The interlayer distance is 9.93 Å. This structural feature resembles those found in the structures of the organic−inorganic assemblies $\{(Hphz)[Fe(CA)_2(H_2O)_2](H_2O)_2\}_n$ (phz = phenazine, CA = chloranilate) and $\{(G)[Co(CA)_2(H_2O)_2]\}_n$ (G = hydroxypyridinium), in which the structures are stabilized by both hydrogen-bonding interactions and electrostatic

(45) Jessen, S. M.; Kuppers, H. *J. Mol. Struct.* **1991**, *263*, 247.

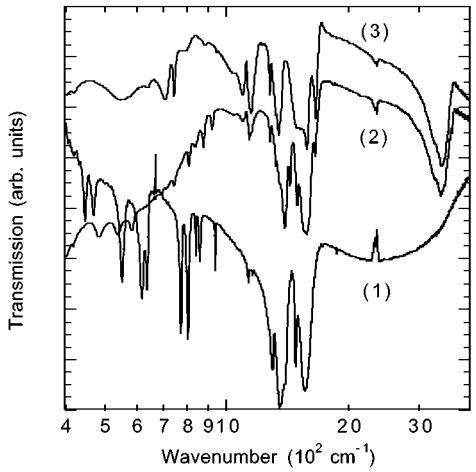

Figure 4. Mid-IR transmission spectra of **1**−**3**.

interactions between the ions.[46] From a magnetic point of view it is worth noting that the cobalt atoms are arranged in a pseudo-triangular array within the layer. However, there are no connections between the metals, and the distances between the cobalt atoms are rather long (6.538, 6.494 and 6.965 Å) for efficient magnetic exchange.

Infrared Spectra. The spectra of the compounds are shown in Figure 4, and their band wavenumbers are given in the Experimental Section. As noted by Jessen et al.[21] and as can also be seen here, the spectra are characteristic of the geometry and coordination environment of the pyromellitate. This is not surprising, considering the many faces of the pyromellitate on coordination (Table 1). In the present cases the pyromellitate in **1** has a mirror bisecting the C−H bonds and a C_2 plane perpendicular to it, in **2** it contains only an inversion center and in **3** it has nearly D_{2h} symmetry. Accordingly, we will only try to rationalize certain observations and compare key features of the three compounds.[47] The bands above 3000 cm^{-1} are assigned to the stretching modes of the water molecules. There are more bands in this region for **2** compared to **3**, due to the presence of both coordinated and noncoordinated water molecules. They are completely absent in **1**. The H−O−H bending modes are observed at ca. 1665 cm^{-1}. Due to the different symmetry and distortions of the C_{10} backbone, its associated bands are at different energies and have different intensities. The bands originating from the carboxylate groups are also complex, due to the presence of hydrogen bonds (intra- and intermolecular) and their different coordination geometries; we can only assign the bands centered about 1380 cm^{-1} to the antisymmetric mode and those at about 1550 cm^{-1} to the symmetric mode. We note the similarity of the coordination mode of the pyromellitate in **1** with those in $Co_2(OH)_2$(terephthalate) and $[M_3(CTC)_2(\mu\text{-}H_2O)_2(H_2O)_2]\cdot 6H_2O$ (M = Ni, Co),[12,15] for which we have drawn an experimental

(46) Kawata, S.; Kumagai, H.; Adachi, K.; Kitagawa, S. *J. Chem. Soc., Dalton Trans.* **2000**, 2409.

(47) (a) Jessen, S. M.; Küppers, H. *J. Mol. Struct.* **1991**, *263*, 247. (b) Deacon, G. B.; Phillips, R. J. *Coord. Chem. Rev.* **1980**, *33*, 227. (c) Nakamoto, K. *Infrared and Raman Spectra of Inorganic and Coordination Compounds*, 5th ed.; Wiley: New York, 1997.

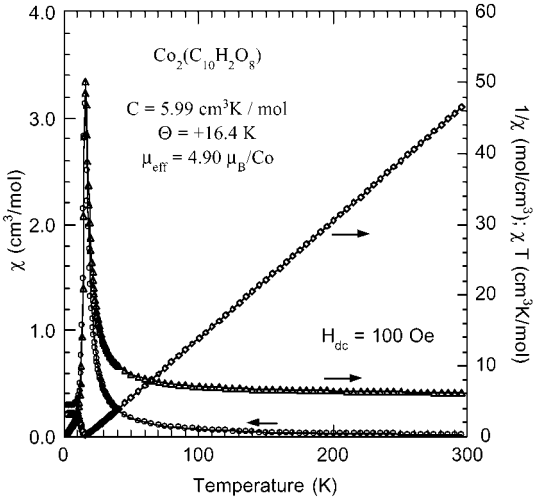

Figure 5. Temperature dependence of χ (circles), χT (triangles), and $1/\chi$ (diamonds) for **1**.

correlation of coordination numbers and energies of the carboxylate bands.

Magnetic Properties. Variable-temperature magnetic susceptibility studies have been performed on polycrystalline samples of **1**−**3** over the temperature range from 2 to 300 K.

The magnetic properties (Figures 5−10) of **1** are quite complex, as it exhibits three different ground states (collinear antiferromagnetism, canted antiferromagnetism, and field-induced ferromagnetism). We shall attempt to present the data to best describe the behavior in the three different temperature regimes. For $T > 20$ K the behavior is that of a paramagnet with Curie constant of 5.99 cm^3 K mol^{-1} and a Weiss constant of +16.4 K for a fit to data taken in an applied field of 100 Oe between 30 and 300 K (Figure 5). This result indicates that ferromagnetic interactions between nearest-neighbor cobalt atoms dominate at high temperatures. The susceptibility increases gradually up to 30 K and then more rapidly toward the maximum at 16 K. There is a sudden drop at 16 K due to long-range antiferromagnetic ordering. The susceptibility tends to a constant value below ca. 12 K; however, its value for $T < 12$ K is only 1/10 of the value at the maximum at T_N and is far from the expected 2/3 for a polycrystalline two-sublattice collinear antiferromagnet.[48] This ratio is similar to that found in $Co_2(OH)_2$(terephthalate),[12] even though the dominant interaction is antiferromagnetic in this case. The susceptibility above 13 K in fields up to 3000 Oe is essentially independent of applied field (Figure 6). Above 3000 Oe it deviates below 50 K, due to the increase of correlation length as a consequence of the ferromagnetic nearest-neighbor exchange.[48]

Magnetization in 1 Oe after zero-field cool (ZFC) and subsequent field cool (FC) in 1 Oe reveals a different behavior and shows that the history of the sample is important (Figure 6a). Above 13 K the magnetization is reversible and behaves similar to that in 100 Oe. Below 13 K there is nonreversibility and bifurcation consistent with a weak spontaneous magnetization due to a second long-range ordering transition. Furthermore, the presence of irreversibility and the zero magnetization at 2 K after zero-field cool

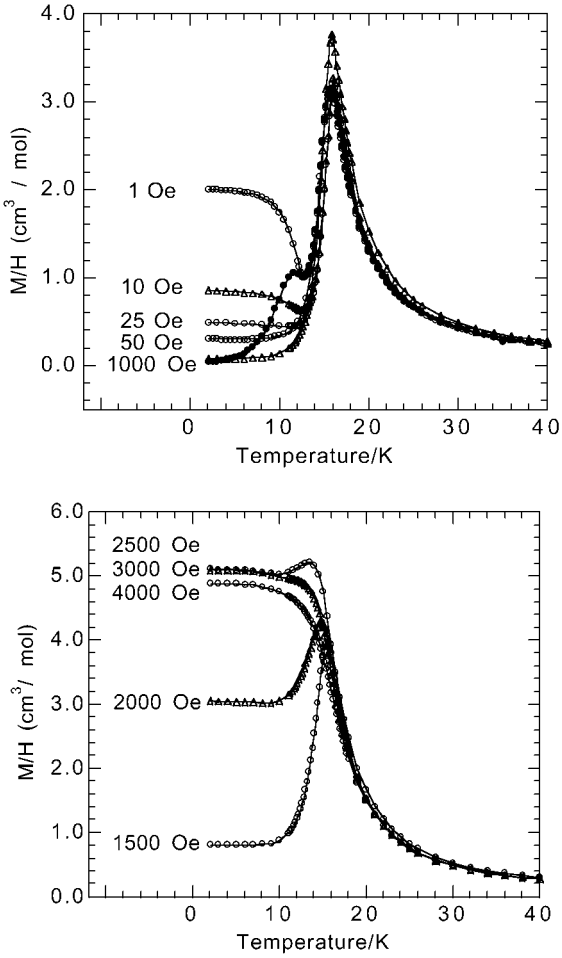

Figure 6. Temperature dependence of the dc magnetic susceptibility (M/H) of **1** in applied fields of (a, top) 1−1000 Oe and (b, bottom) 1500−4000 Oe taken in field cooling mode. The data in 1 Oe were taken after zero-field cooling to 2 K and show the bifurcation point at 12.8 K. For clarity the data taken on warming are shown as filled circles.

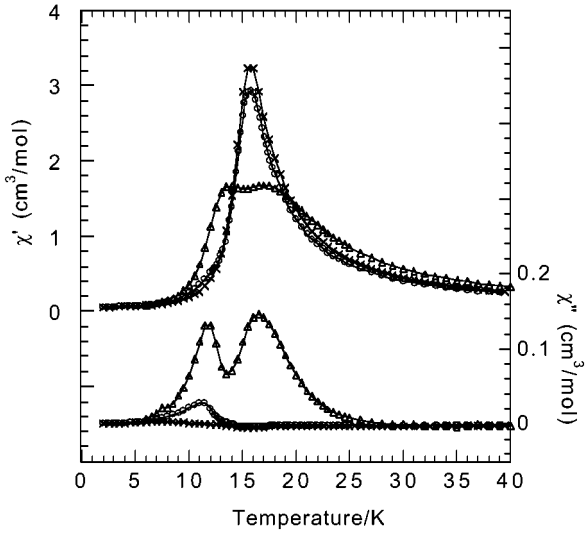

Figure 7. Temperature dependence of the ac magnetic susceptibilities of **1** measured in a field amplitude of 1 Oe (20 Hz) and a dc bias field of 1 Oe (circles), 100 Oe (plus signs), and 4 kOe (triangles).

(48) Herpin, A. *Theorie du Magnetisme*; Presse Universitaire de France: Paris, 1968.

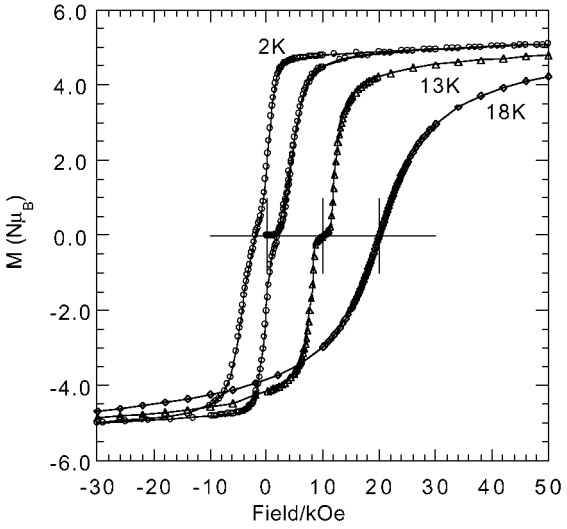

Figure 8. Isothermal magnetization of **1** measured in the paramagnetic region at 18 K (diamonds), in the collinear antiferromagnetic region at 13 K (triangles), and in the canted AF/ferromagnetic region at 2 K (circles). For clarity we have offset the data at 13 and 18 K by 10 and 20 kOe, respectively.

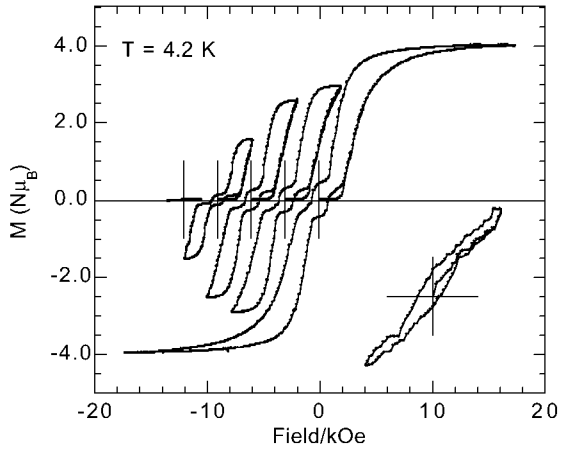

Figure 9. Virgin magnetization and hysteresis loops of **1** at 4.2 K in different upper magnetic field limits (1500, 3000, 4000, 5000, and 18 000 Oe) after ZFC. Note that the virgin magnetization is outside the hysteresis loops.

suggest the presence of a multidomain microstructure within the crystals.[49] The weak magnetization appears to be saturated in this low field of 1 Oe, as is commonly found for canted antiferromagnets.[50] From the saturation value in 1 Oe at 2 K, we estimate the canting angle to be 0.002°. The temperature dependence of field cool measurements in different applied fields indicates that the canting angle remains unperturbed up to 1000 Oe (Figure 6a). For fields exceeding 1500 Oe (Figure 6b), the magnetization increases below 13 K, while it remains reversible above. This suggests that the moments of the sublattices rotate proportionally to the strength of the applied field up to about 3000 Oe, where it

(49) (a) Chikazumi, S. *Physics of Ferromagnetism*; Oxford University Press: Oxford, U.K., 1992. (b) Bertotti, G. *Hysteresis in Magnetism*; Academic Press: London, 1998.

(50) (a) Rettig, S. J.; Storr, A.; Summers, D. A.; Thompson, R. C.; Trotter, J. *J. Am. Chem. Soc.* **1997**, *119*, 8675. (b) Banister, A. J.; Brincklebank, N.; Lavender, I.; Rawson, J. M.; Gregory, C. I.; Tanner, B. K.; Clegg, W.; Elsegood, M. R. J.; Palacio, F. *Angew. Chem., Int. Ed. Engl.* **1996**, *35*, 2533.

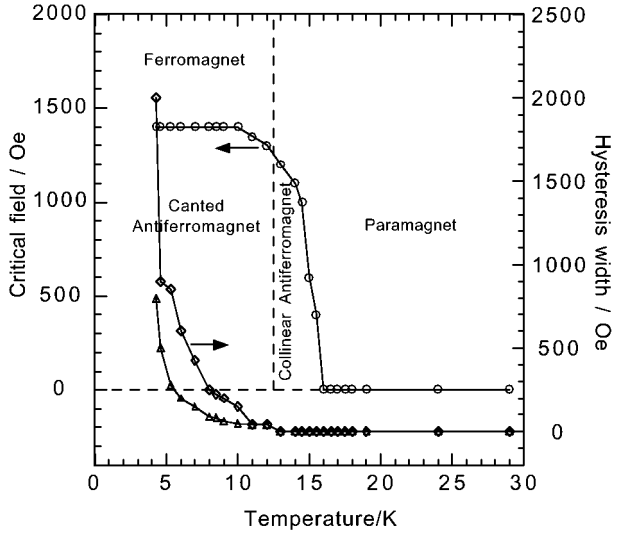

Figure 10. *H*−*T* phase diagram for **1**: temperature dependence of the critical field after ZFC (circles), the width of the hysteresis loop centered at zero field (triangles), and the width of the loop at the critical metamagnetic field (diamonds).

starts to saturate to a value approaching the expected moment per cobalt(II). We note that the saturation magnetization is 80 emu/g of compound. This value is very high for a molecular system and is larger than that of metallic Ni (55 emu/g) and garnets (ca. 60 emu/g), comparable to those of ferrites (ca. 75 emu/g), and lower than those of metallic Fe (220 emu/g) and Co (160 emu/g).[48]

The ac magnetization was measured in an ac field of amplitude 1 Oe oscillating at 20 Hz in three different dc bias applied fields of 1, 100, and 4000 Oe in the temperature range 2−40 K (Figure 7). In the applied field of 1 Oe the in-phase component of the susceptibility (χ') exhibits a maximum at 16 K and a weak shoulder at ca. 12 K. The out-of-phase component (χ'') exhibits only one peak at 12 K; its nonzero value is at 14 K. We did not observe hysteresis in the ZFC−FC data in 1 Oe. This is consistent with the picture described above. In 100 Oe, only the maximum in χ' is observed; neither the shoulder at 12 K nor the peak in χ'' is present. In 4 kOe, there are two maxima in both χ' and χ'' at 17 and 11 K. The value at the maximum at 17 K is approximately half that in 1 or 100 Oe applied field, while the value at 12 K is about 4 times the corresponding value in 1 Oe. This gain in χ'' at the expense of χ' would be consistent with the presence of magnetocrystalline anisotropy and the increase of correlation length on increasing the measuring applied field.[49a] It is quite surprising to see a large out-of-phase component in the paramagnetic region and within the collinear antiferromagnetic region (12−16 K). One possible explanation of this would be that the compound is behaving as a superparamagnet in this field and the anisotropic field retards the oscillation of the moments in such small field amplitudes of 1 Oe and a frequency of 20 Hz. Measurements performed in zero dc bias field and a field of amplitude 1 Oe oscillating at different frequencies (1−1000 Hz) show no frequency dependence (see Supporting Information, Figure S8). Further measurements in different

amplitudes and at different frequencies would be needed to advance our understanding of the physics of this effect.

Isothermal magnetization has been measured at several temperatures and field ranges employing different experimental protocols. Data taken after ZFC are shown in Figures 8 and 9. Above 25 K the magnetization is almost linear, as expected for a paramagnet, and Brillouin type behavior is observed for $16 < T < 25$ K in accordance with short-range correlation. Between T_N and $T_{canting}$ ($12 < T < 16$ K) a characteristic reversible metamagnetic behavior is observed with a critical field increasing as the temperature is lowered. Below $T_{canting}$, hysteresis sets in and its width widens as the temperature is lowered (Figure 10). Two different loops are observed: one around zero field and the other around the critical metamagnetic field. The phase diagram characterized by the temperature dependence of the critical field after ZFC is shown in Figure 10 together with the widths of the hysteresis loops. The critical field increases to a maximum of 1500 Oe below 10 K as the temperature is lowered. In Figure 9, we show the hysteresis at 4.2 K after ZFC from 30 K for different limiting upper applied fields. When the applied field is ramped to a maximum, that is, below the critical field (H_c), the magnetization is almost reversible. There is a very small loop with a remanence of 0.006 μ_B and a coercive field of 200 Oe (inset of Figure 9). When the applied field was increased above H_c but below the field at which the magnetization saturates, we observed the two loops described above with constant hysteresis widths but of proportional magnetization to the maximum applied field. From this we can infer that the two loops are intrinsic and they are related to the same effect. Whether they belong to different crystal orientations remains an unanswered question to date. The remanance magnetization was measured after cooling the sample in a field of 5 T to 2 K and the measurements performed in zero applied field on warming. There is a large drop in magnetization between 2 and 3 K followed by a slow reduction up to the 12 K (Supporting Information, Figure S9). Above 12 K, there is no remanance magnetization. While the large drop below 3 K is due to the rapid decrease of the hysteresis width of the loop centered at the metamagnetic transition, the slow drop is due to the slow decrease of the loop centered about zero field. This behavior is the same as that observed for $Co_2(OH)_2$(terephthalate).[12] For the latter saturation of the remanance magnetization is observed below 20 K due to the wide hysteresis width.

Figure 11 displays the temperature dependence of the inverse susceptibility and the product of susceptibility and temperature of **2** and **3**. The magnetic behaviors are similar in the two cases: viz. the χT value decreases as the temperature is lowered. **2** exhibits a Curie−Weiss behavior with a Weiss constant of −20.8(1) K and Curie constant of 7.00(3) cm^3 K mol^{-1}. The calculated effective magnetic moment (μ_{eff}) per cobalt is 5.29 μ_B. **3** behaves as a Curie−Weiss paramagnet above 50 K and a fit to the data in the temperature range 150−300 K gives a Weiss constant of −19.9(6) K and a Curie constant of 2.95(1) cm^3 K mol^{-1}. The calculated effective magnetic moment (μ_{eff}) per cobalt

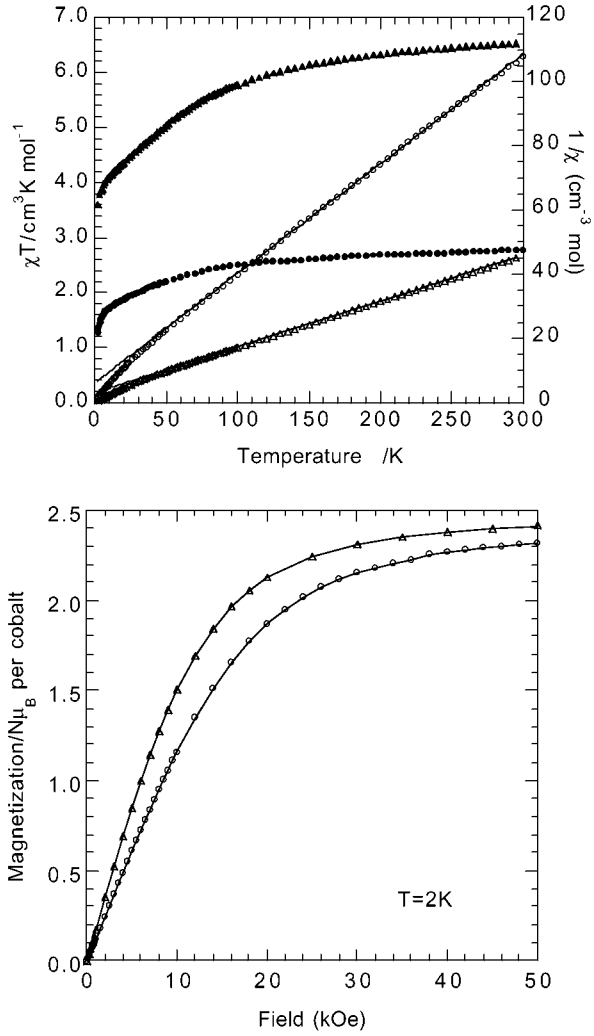

Figure 11. (a, top) Temperature dependence of $1/\chi$ (open symbols) and χT (filled symbols) for **2** (triangles) and **3** (circles). (b, bottom) Isothermal magnetization at 2 K for **2** (triangles) and **3** (circles).

ion is 4.86 μ_B, which is within the range expected for an octahedral cobaltous ion. The larger value for **2** may be due to the low symmetry of the octahedron in **2** compared to **3**, resulting in a small change in the value of 10*Dq* and the observed red color of the compound.[44] The negative Weiss constant is due to the effect of spin−orbit coupling, resulting in a gradual transformation of an isotropic $s = {}^3/_2$ at high temperature to an anisotropic $s_{eff} = {}^1/_2$ at low temperature. The value of −20 K is exactly that expected for an isolated Co(II) with a spin−orbit constant of 170 cm^{-1}.[51] No antiferromagnetic exchange interaction between nearest-neighbor cobalt ions can be observed. Isothermal field dependence magnetization of **2** and **3** at 2 K increases gradually to 2.4 and 2.3 μ_B per cobalt, respectively, at 5 T. The values are consistent with those expected for a polycrystalline sample of Co(II) ion with an effective $s = {}^1/_2$ and an anisotropic *g* value.

Heat Capacity of 1. The experimental heat capacity/temperature (C_p/T) is shown in Figure 12. In the absence of a nonmagnetic analogue of the compound we carried out an

(51) Mabbs, F. E.; Machin, D. J. *Magnetism and Transition Metal Complexes*; Chapman and Hall: London, 1973.

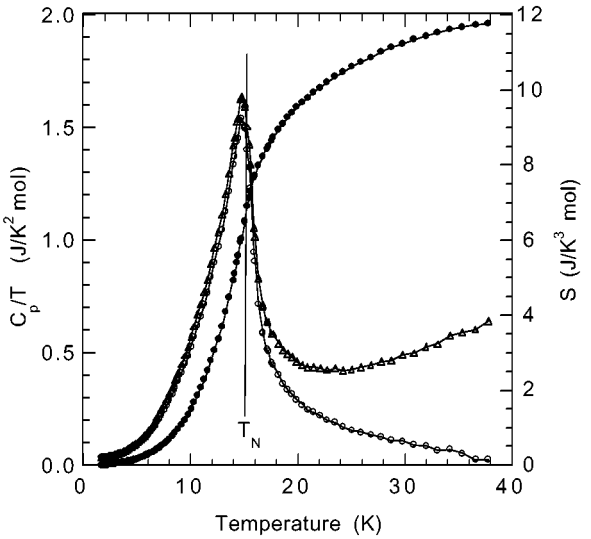

Figure 12. Plot of the heat capacity/temperature (C_p/T) of **1** as a function of temperature as measured (triangles) and after correction for the electronic contribution (circles) and the integrated magnetic entropy (filled circles).

electronic background correction by subtracting an AT^3 term to give the magnetic contribution. The value of A was fixed to give no magnetic contribution well above the magnetic transition at 40 K. The sharp peak at the transition and the absence of any Schottky background in the heat capacity suggest the compound has a 2D or 3D magnetic dimensionality.[52] The magnetic entropy was derived by integration of the C_p/T versus T plot up to 40 K. It increases continuously to T_N and then monotonically up to 40 K. The value of the entropy approaches 12 J/(K mol) (6 J/K per cobalt). This value is only half of the expected 23 J/(K mol) (11.5 J/K per Cobalt) for $2R \ln(2s + 1)$ if $s = {}^3/_2$. However, since cobalt is known to have $s_{eff} = {}^1/_2$ at low temperatures,[53] the value of 12 J/(K mol) is in good agreement with the expected 11.5 J/(K mol) for $2R \ln(2s + 1)$ and $s = {}^1/_2$. An important point regarding the dimensionality of this compound is that only 60% of the entropy is acquired up to the transition temperature. This is consistent with a 2D rather than a one 1D or 3D magnetic system. The continuous increase of the entropy above T_N also suggests that an appreciable short-range order persists from T_N to well above 35 K. This short-range order is in good agreement with the low dimensionality.

Summary

The chemistry of transition metals with pyromellitate as a ligand is not as simple as expected. The various stable charges, geometries, and modes of coordination provide a wealth of compounds with very diverse structures and properties. The enhanced thermal stability compared to other metal carboxylates is dictated by the number of coordinate bonds and the number of coordination metals that leave no available coordination sites for water. The spectra in the mid-infrared region are characteristic of the different geometries and symmetries of the pyromellitate.

From a magnetic point of view, compounds **2** and **3** are not as interesting, due to the large distances between the magnetic centers and the weak interactions (hydrogen bonding and O−C−O bridges). Compound **1**, on the other hand, exhibits a very unusual magnetic behavior, with three ground states (collinear and canted antiferromagnetism and field-induced ferromagnetism). To rationalize these observations, we can use the Goodenough[54] and Kanamori[55] rules for superexchange mechanism as a starting point. Three magnetic exchange pathways can be defined in **1**. The first, and possibly the strongest, is the exchange between cobalt atoms in the chains that are 3.363 Å apart and are connected by two single bridges consisting of an oxygen atom each. The Co−O−Co angle of 103.8° and the CoO_2Co flatness (torsion angle of 0.2°) can give rise to either ferromagnetic or antiferromagnetic interactions. From the observed positive Weiss temperature, we assign this exchange to be ferromagnetic. The second in the hierarchy is the exchange between the chains via the O−C−O bridges at a distance of 4.475 Å for Co−O−C−O−Co. From previous observations in other known compounds we know that this exchange is weak and possibly antiferromagnetic in character. The last is that between the layers that involved the benzene backbone. The distance is 8.8 Å, and the path is via $O-C_4-O$ bridges. This interaction is therefore weaker than the second one. To account for the collinear antiferromagnetic ordering at 16 K, two scenarios can be envisaged. One is that the arrangement of the moments is antiparallel ferromagnetic chains and the second is antiparallel ferromagnetic layers. The present observations together with those for the series $Co_2(OH)_2$-(dicarboxylate)[12] (where the dicarboxylate is terephthalate, naphthalenedicarboxylate, carboxycinnamate, or biphenyldicarboxylate in increasing length) tend to support the latter. For the hydroxide compounds we have demonstrated that the Néel temperature is weakly dependent on the interlayer distance, while the critical metamagnetic field is very dependent. We interpreted this observation as follows: the Néel temperature is independent due to the similarity of the layers, where only one exchange pathway is defined by Co−O−Co in the different compounds, while the critical field scales with the interlayer exchange interactions. In the present case, the ferromagnetic layers are slightly weakened by the combination of two different pathways, Co−O−Co and Co−O−C−O−Co, which results in a lowering of T_N compared to the Co−OH layered compounds. However, the critical field of ca. 3000 Oe for **1** (interlayer distance 8.8 Å) is marginally lower than for $Co_2(OH)_2$(terephthalate) (interlayer distance 9.9 Å), consistent with similar interlayer exchange energies for the two compounds.[12]

The unusual features characterizing this novel class of antiferromagnets are (a) the two well-separated long-range ordering events, collinear and canted antiferromagnetism, and (b) the double-hysteresis loops.[12] Their presence in three

(52) Takeda, S. Private communication (University of Kyushu).
(53) De Jongh, L. J., Ed. *Magnetic Properties of Layered Transition Metal Compounds*; Kluwer Academic: Dordrecht, The Netherlands, 1990.
(54) Goodenough, J. B. *Magnetism and the Chemical Bond*; Wiley: New York, 1963.
(55) (a) Kanamori, J. *J. Phys. Chem. Solids* **1959**, *10*, 87. (b) Kanamori, J. In *Magnetism*; Rado, G. T., Suhl, H., Eds.; Academic Press: New York, 1963; Vol. I, Chapter 4, p 127.

structurally different compounds of cobalt raises the question of what stabilizes these particular ground states. The origin of the canting in these compounds is still a mystery. The canting is derived from neither the antisymmetric exchange mechanism of DM,[56] as the symmetry of the lattice is high, nor the different anisotropic metal centers, as suggested by Moriya[57] for NiF_2. It cannot be derived from a difference of *g* values of the magnetic centers in the different sublattices, since **1** contains only one crystallographically independent cobalt atom in the cell. It is also not a structural effect, for we observe identical effects for three structurally different compounds. We are left to think that this effect may be a property of octahedral Co(II). It is not surprising that more examples are not found in the literature, given that most magnetic studies dealing with molecular systems are performed in fields in excess of 100 Oe. In the absence of a neutron diffraction study we can only speculate on the magnetic structure of **1**. One proposition is there are several magnetic sublattices with their moments arranged like a flat umbrella. The ordering of their moments in a symmetric fashion gives the collinear AF ground state, and a slight asymmetry in the radial vectors at $T_{canting}$ results in the very small spontaneous magnetization. Application of a field first flips oppositely oriented cones to point in the same direction at the critical field and then closes the moments in the cones to eventually aligning them all parallel.[58] Thus, the linear increase of the magnetization in fields is larger than the critical field.

The range of structures, due to both hydrogen-bonding interactions and coordination bonds, found with cobalt suggests that the coordination chemistry of pyromellitate ions is a rich field to be explored. Due to the lack of efficient magnetic exchange in compounds **2** and **3**, they behave as paramagnets. An unusual magnetic behavior is observed for **1**, which is only known for two other structural types,[12,13] raises the question of whether it is specific to Co(II).[59] This new magnetic phenomenon adds to the number of unusual and unexplained magnetic behaviors exhibited by molecular systems.[60]

Acknowledgment. This work was funded by the CNRS-France, the Australian Research Council, and the JSPS-Japan. H.K. thanks the JSPS for a Young Scientist Fellowship for his stay in Strasbourg. and M.K. thanks the Royal Society of Chemistry for a travel grant. We thank Drs. A. De Cian and N. Kyritsakas and J. L. Rehspringer (Strasbourg).

Supporting Information Available: Tables giving selected bond distances and angles for **1**−**3** and figures giving additional views of **1**−**3** and additional characterization data. This material is available free of charge via the Internet at http://pubs.acs.org.

IC020065Y

(56) (a) Dzyaloshinsky, I. *J. Phys. Chem. Solids* **1958**, *4*, 241. (b) Moriya, T. *Phys. Rev.* **1960**, *120*, 91.
(57) Moriya, T. In *Magnetism*; Rado, G. T., Suhl, H., Eds.; Academic Press: New York, 1963; Vol. I, Chapter 4, p 85.
(58) (a) Day, P. *Acc. Chem. Res.* **1988**, *21*, 250. (b) Stryjewski, E.; Giordano, N. *Adv. Phys.* **1997**, *26*, 487. (c) Aruga Katori, H.; Katsumata, K. *Phys. Rev. B* **1996**, *54*, R9620.
(59) Caneschi, A.; Gatteschi, D.; Lalioti, N.; Sangregorio, C.; Sessoli, R.; Venturi, G.; Vindigni, A.; Rettori, A.; Pini, M. G.; Novak, M. A. *Angew. Chem., Int. Ed.* **2001**, *40*, 1760.
(60) (a) Kaul, B. B.; Durfee, W. S.; Yee, G. T. *J. Am. Chem. Soc.* **1999**, *121*, 6862. (b) Zhao, H.; Clérac, R.; Sun, J.-S.; Ouyang, X.; Clemente-Juan, J. M.; Gómez-García, C. J.; Coronado, E.; Dunbar, K. R. *J. Solid State Chem.* **2001**, *159*, 281−292. (c) Ohkoshi, S.-I.; Hashimoto, K. *J. Am. Chem. Soc.* **1999**, *121*, 10591. (d) Manriquez, J. M.; Yee, G. T.; McLean, R. S.; Epstein, A. J.; Miller, J. S. *Science* **1991**, *252*, 1415. (e) Miller, J. S. *Inorg. Chem.* **2000**, *39*, 4392.